PHYSICAL REVIEW B **81**, 140204(R) (2010)

Coupling between chemical and dynamic heterogeneities in a multicomponent bulk metallic glass

T. Fujita,[1] P. F. Guan,[1] H. W. Sheng,[2] A. Inoue,[1] T. Sakurai,[1] and M. W. Chen[1,*]
[1]*WPI Advanced Institute for Materials Research, Tohoku University, Sendai 980-8577, Japan*
[2]*Department of Computational and Data Sciences, George Mason University, Fairfax, Virginia 22030, USA*
(Received 3 March 2010; published 28 April 2010)

We performed molecular-dynamics simulation and predicted a strong coupling between chemical short-range order and dynamic heterogeneity in a multicomponent $Cu_{45}Zr_{45}Ag_{10}$ alloy that possesses excellent glass-forming ability. The intrinsic correlation between the chemical and dynamic heterogeneities leads to significant spatial partitioning and dynamic isolation between Cu-rich slow-dynamics regions and Ag-rich fast-dynamics regions. This characteristic may play an important role in the improved glass-forming ability with Ag addition by retarding crystallization kinetics.

DOI: 10.1103/PhysRevB.81.140204 PACS number(s): 64.70.pe, 61.43.−j, 83.10.Rs

The formation of metallic glasses usually requires rapid cooling in order to freeze the disordered structure of metal melts.[1] Recently, numerous multicomponent alloys have been discovered to possess an unusual capability of forming bulk metallic glasses (BMGs) at a very low cooling rate.[2] In view of the thermodynamic relationship between structure and phase stability in crystalline materials, the atomic origins of BMG formation have been intensively discussed from a geometrical and topological perspective of the dense atomic packing.[3–9] Because BMGs are out-of-equilibrium systems, their formation involves structural evolution in time and thus cannot be studied in terms of thermodynamics alone.[10,11] In general, a superior glass former exhibits slow dynamics and a long α relaxation time at a temperature above glass transition point, T_g. This concept has been used to empirically explain the alloying effect in the improved glass-forming ability (GFA) of various glassy materials.[12–15] Nevertheless, the intrinsic correlation of the dynamic process with atomic structure and chemistry of metallic glasses has not been well elucidated. In this study, we performed molecular-dynamics simulation in order to investigate the dynamics of a multicomponent supercooled liquid. We predicted a strong coupling between chemical short-range order and dynamic heterogeneity in a $Cu_{45}Zr_{45}Ag_{10}$ BMG, which may offer dynamic insights on the metallic glass formation of multicomponent alloys.

An open code software for molecular dynamics simulation, LAMMPS,[16] was employed to investigate the dynamic process of $Cu_{45}Zr_{45}Ag_{10}$ and $Cu_{50}Zr_{50}$. The many-body potentials used in the calculations were developed using the embedded atom method (EAM) on the basis of the *ab initio* calculations derived from the Vienna *ab initio* simulation package (VASP). A force-matching method was used to fit the predetermined potential energy landscapes.[6] The reliability and accuracy of the EAM potentials have been experimentally assessed previously.[9] Eight thousand atoms ensemble for both $Cu_{45}Zr_{45}Ag_{10}$ and $Cu_{50}Zr_{50}$ were melted at 2500 K for 0.1 ns (with a time step of 5 fs) and then cooled to 300 K at various cooling rates.[17] The atomic configurations were analyzed by grouping the nearest-neighbor environments of each atom as Voronoi polyhedra[18] and the dynamic process was characterized by tracking the atomic positions during relaxation at 800 K, i.e., ~100 K above T_g.

In both liquid and glass states, chemical inhomogeneity can be observed in $Cu_{45}Zr_{45}Ag_{10}$, which is composed of Cu-rich clusters centered by Cu atoms and Zr- and Ag-enriched interpenetrating clusters centered by Ag pairs or chains.[9] Atomic structure evolution during cooling at a quenching rate of 2×10^{10} Ks^{-1} is shown in Fig. 1(a). We examined the fraction of Voronoi indexes of the representative Cu-centered polyhedra and the average number of the neighboring Ag atoms in Zr-rich interpenetrating clusters. As the temperature approaches T_g (~700 K), the population of Cu-centered $\langle 0,0,12,0\rangle$ icosahedral short-range order (ISRO) clusters and the average number of neighboring Ag atoms in the form of strings increases dramatically. Figure 1(b) shows a cross section of the atomic structure observed at 300 K; only the Cu atoms in the $\langle 0,0,12,0\rangle$ polyhedra and Ag atoms are displayed. In this figure, the interpenetrating clusters centered by the stringed Ag atoms are traced with dotted lines. The average number of Ag atoms in the Cu-centered $\langle 0,0,12,0\rangle$ polyhedra is only 0.65, whereas the average number of Ag atoms in the Ag-centered interpenetrating clusters is 2.7 without counting the center Ag atoms.

In order to investigate the dynamics of the supercooled liquids, the 8000 atoms ensemble of $Cu_{45}Zr_{45}Ag_{10}$ and $Cu_{50}Zr_{50}$ were adequately relaxed at 800 K and the atomic configurations were used to initialize the individual atom positions. We tracked the atomic structure evolution of the supercooled liquids during relaxation. As shown in the supplemental information,[17] the fractions of both the Cu-centered $\langle 0,0,12,0\rangle$ clusters and Ag-centered interpenetrating clusters in $Cu_{45}Zr_{45}Ag_{10}$ stay dynamically stable during the relaxation, i.e., the individual clusters change with the relaxation time whereas their statistic distribution remains near constant. It is known that the decay of density fluctuations can be described by the self-intermediate scattering function (SISF), $F_s(\mathbf{q},t)=(\sum_{j=1}^{N_a}\exp[i\mathbf{q}\cdot\Delta\mathbf{r}_j(t)])/N_a$, where N_a denotes the number of atoms and $\Delta\mathbf{r}_j(t)=\mathbf{r}_j(t)-\mathbf{r}_j(0)$ is the displacement vector. The α relaxation time t_α is defined as the time interval in which $F_s(\mathbf{q},t_\alpha)=e^{-1}$. The value of wave vector $\mathbf{q}$ is fixed at $|q_{max}|$, which corresponds to the first peak of the partial structure factor of a specific element $\boldsymbol{a}$ in a multicomponent alloy system. The comparison between the SISF of $Cu_{45}Zr_{45}Ag_{10}$ and $Cu_{50}Zr_{50}$ glasses is shown in Fig. 2(a). Although the GFA of $Cu_{45}Zr_{45}Ag_{10}$ is significantly better than that of $Cu_{50}Zr_{50}$,[19] the relaxation dynamics of Cu and Zr

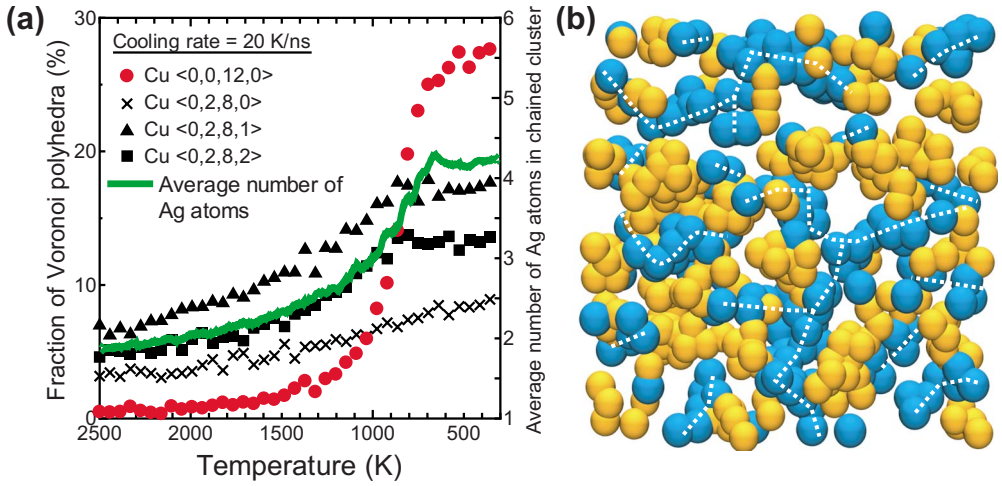

FIG. 1. (Color online) (a) Temperature dependence of a fraction of dominant Voronoi polyhedra centered by Cu atoms in $Cu_{45}Zr_{45}Ag_{10}$ during cooling from 2500 to 300 K. The average number of Ag atoms in Ag-chained clusters is also plotted against temperature. (b) Cross section of atomic structure of glassy $Cu_{45}Zr_{45}Ag_{10}$ at 300 K. The bronze (light gray in printed version) and dark blue (dark gray) balls represent Cu and Ag atoms, respectively. The Cu atoms center the polyhedra with a Voronoi index $\langle 0,0,12,0\rangle$. Zr atoms are not shown in order to clearly illustrate the chemical heterogeneity.

in the binary and ternary systems are surprisingly very similar and t_α of Cu and Zr in both systems falls in the range of 0.2–0.5 ns. Moreover, the relaxation dynamics of Ag are even faster than those of Cu and Zr. Generally, the enhanced GFA is associated with the slow structural relaxation. For instance, in $Cu_{46}Zr_{47}Al_7$, the presence of Al results in a high magnitude of t_α of Cu and Zr as compared to that in a $Cu_{46}Zr_{54}$ binary alloy.[13] Therefore, the fact that Ag does not induce a pronounced slowdown in the dynamics of $Cu_{45}Zr_{45}Ag_{10}$ is in obvious disagreement with the experimental observation that the glass-forming ability of the ternary system exhibits a dramatic improvement with the addition of 10 at. % Ag.[19] With the aim of exploring the dynamic mechanism behind the effect of Ag on the enhanced GFA, we analyzed the dynamic susceptibility, which is correlated with the dynamic heterogeneity, of $Cu_{50}Zr_{50}$ and $Cu_{45}Zr_{45}Ag_{10}$ using the equation[20]

$$\chi_4(t) = N\left[\left\langle\left(\left\{\sum_{j=1}^{N}\exp[i\mathbf{q}\cdot\Delta\mathbf{r}_j(t)]\right\}/N\right)^2\right\rangle - \left\langle\left\{\sum_{j=1}^{N}\exp[i\mathbf{q}\cdot\Delta\mathbf{r}_j(t)]\right\}/N\right\rangle^2\right],$$

where $N=8000$ at 800 K. Because the peak height at t_α is approximately proportional to the square of the dynamic correlation length,[21,22] we can conclude from Fig. 2(b) that the atomic motion in $Cu_{45}Zr_{45}Ag_{10}$ becomes less cooperative than that in the binary $Cu_{50}Zr_{50}$. Although the addition of Ag does not change the relaxation time of Cu and Zr considerably, it notably increases the dynamic heterogeneity of $Cu_{45}Zr_{45}Ag_{10}$.

To study the spatial distribution of the $Cu_{45}Zr_{45}Ag_{10}$ dynamic heterogeneity in short and long dynamic propensity of motion at 800 K, isoconfiguration was conducted 1000 times using the same initial configuration and an independent random distribution of initial momenta over a fixed time interval.[23] For the short-time dynamic propensity, the time interval is approximately 1.5 times the β relaxation time, t_β, at which the non-Gaussian parameter $(3\langle\Delta\mathbf{r}^4(t)\rangle/5\langle\Delta\mathbf{r}^2(t)\rangle^2)-1$ is maximum. The mean-square displacements for each isoconfiguration were measured and averaged for each atom in order to correlate the local atomic environments with the measured displacements. The atomic displacements of the Cu atoms were sorted in an increasing order and divided into 20 groups. The fraction of the Cu-centered full icosahedra and the number of coordinated Ag atoms in each group are plotted against atomic mobility for a short time interval in Fig. 3(a). Interestingly, a high ISRO cluster population and Ag-fewer environments are responsible for slow dynamics. In contrast, a low ISRO cluster population and Ag-rich environments correspond to fast dy-

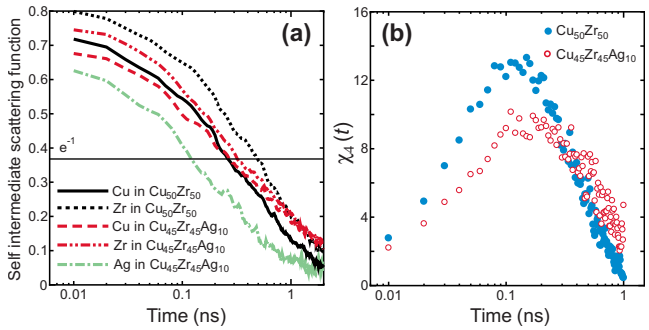

FIG. 2. (Color online) (a) Self-intermediate scattering functions of Cu, Zr, and Ag in $Cu_{50}Zr_{50}$ and $Cu_{45}Zr_{45}Ag_{10}$ liquids. (b) Dynamic susceptibility of $Cu_{50}Zr_{50}$ and $Cu_{45}Zr_{45}Ag_{10}$ as function of time.

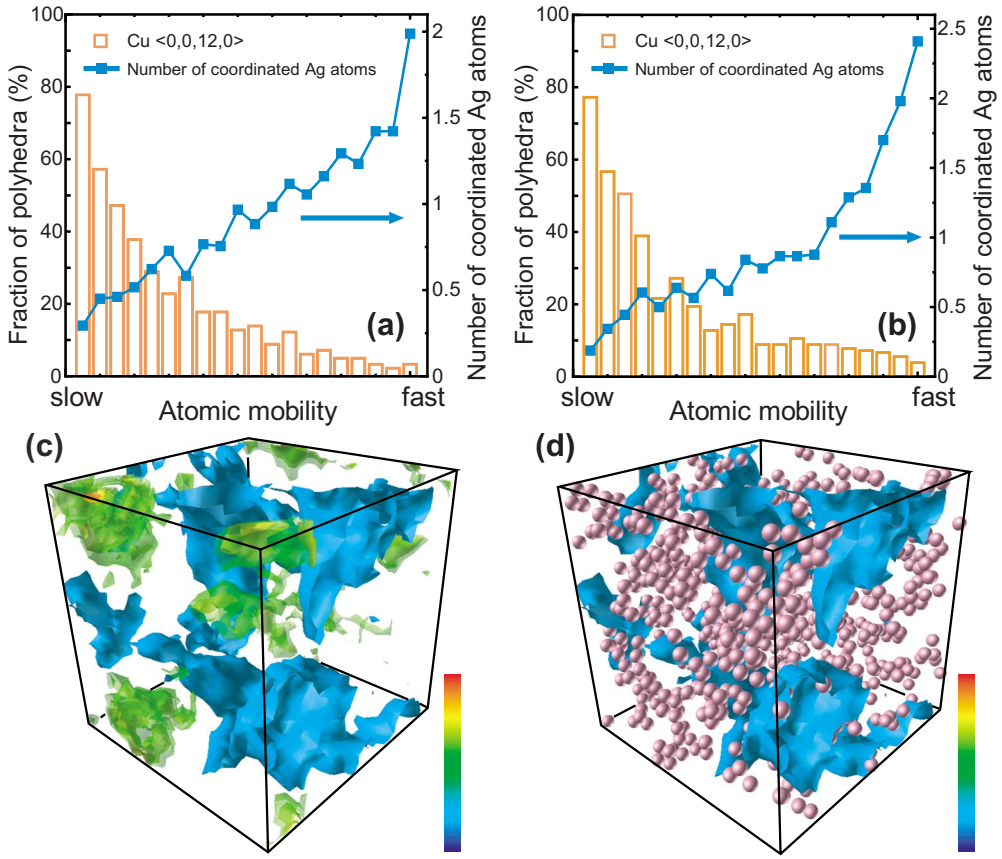

FIG. 3. (Color online) Correlation between atomic mobility of Cu atoms and their local structural environments in $Cu_{45}Zr_{45}Ag_{10}$ at 800 K. The Cu atoms are sorted into 20 groups in the increasing order of their displacement. In each group, the percentage of $\langle 0,0,12,0\rangle$ polyhedra and the number of coordinated Ag atoms are plotted with (a) a short time interval of $1.5t_\beta$ and (b) a long time interval of $1.5t_\alpha$. (c) 3D mean-square displacement map of all atoms based on propensity motion for the conditions observed in (b). The isosurfaces indicate the slow- and fast-dynamics regions where Δr^2 is less than 25 Å^2 (blue regions, dark gray in printed version) and more than 80 Å^2 (green to red regions, light gray to gray), respectively. (d) 3D map showing both isosurfaces of slow-dynamics regions and distribution of Ag atoms (balls). The slow-dynamics regions are apparently Ag-poor regions. The cube has the dimensions of $53\times53\times53$ Å^3; the color bars shown in (c) and (d) show the range from fast (top) to slow (bottom) dynamics.

namics. The displacement measurements of the Zr atoms also demonstrate that the Zr atoms in Ag-rich regions exhibit faster dynamics compared to those in Ag-fewer regions. For the long-time dynamic propensity with a time interval of $1.5t_\alpha$, a similar result was obtained, as shown in Fig. 3(b). Moreover, the composition of local clusters in the slowest and fastest groups shown in Fig. 3(b) were determined to be $Cu_{55}Zr_{44}Ag_1$ (at. %) and $Cu_{35}Zr_{45}Ag_{20}$, respectively. Both the long-time (α process) and short-time (β process) dynamic heterogeneities[24] are closely correlated with the atomic-scale inhomogeneity in the structure and chemistry of the BMG. Figure 3(c) shows a three-dimensional (3D) displacement map with dimensions of $53\times53\times53$ Å^3 that visualizes the isosurfaces of slow-dynamic regions where Δr^2 is less than 25 Å^2 and fast-dynamics regions where Δr^2 is greater than 80 Å^2. The slow- and fast-dynamics regions, corresponding to Ag-poor and Ag-rich regions, respectively, appear to be partitioned from each other. The correlation between dynamic heterogeneity and chemical inhomogeneity is further confirmed by Fig. 3(d), in which both isosurfaces of slow dynamics regions and Ag atoms are illustrated. Again, it can be observed that the slow-dynamics regions contain fewer Ag atoms.[17]

We attempted to analyze the structural origins and relaxation process in terms of the potential-energy landscape (PEL) by means of a distance matrix (DM) $\Delta^2(t,t') = \frac{1}{N}\Sigma_{i=1}^{N}|\mathbf{r}_i(t)-\mathbf{r}_i(t')|^2$, where $\mathbf{r}_i(t)$ is the position of atom i at time t along a single trajectory.[25] The initial positions of the fastest 180 and slowest 180 Cu atoms shown in Fig. 3(b) were selected. Figure 4(a) shows the DM for the group of slowest Cu atoms. This DM clearly indicates the transition between local minima in the PEL or the so-called metabasin (MB) transition. In contrast, the DM for the group of fastest Cu atoms does not indicate the MB-MB transition [Fig. 4(b)]. Accordingly, the cooperative rearranging region (CRR) (Ref. 26) corresponding to the rich ISRO regions can be clearly recognized. The Ag-chained clusters and the neighboring atoms outside the CRR do not contribute to the dynamics inside the CRR. It appears that the heterogeneous dynamics are due to inactive domains with rich ISRO regions and active domains with a high Ag content. The shortened dynamic correlation length caused by the addition of Ag [Fig. 2(b)] can be reasonably explained by geometrically partitioning the ISRO regions with the Ag-chained clusters, as shown in Fig. 3(c). The glass formation of an alloy during rapid cooling is a competitive process between the stability

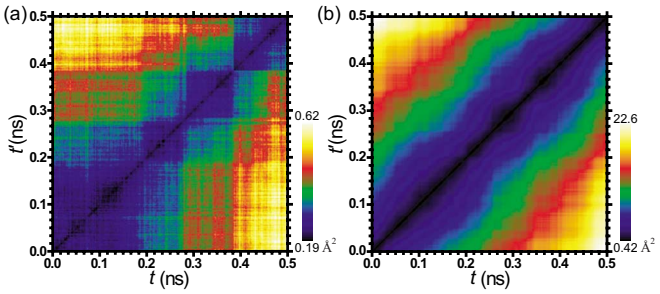

FIG. 4. (Color online) Distance matrix for (a) the slowest and (b) the fastest Cu atoms categorized in Fig. 3(b). Darker squarelike areas in (a) correspond to the atoms that travel a smaller distance and indicate the MB-MB transitions. These transitions are not observed for the fastest Cu atoms.

of a supercooled liquid and the kinetics of crystallization. Because crystallization requires long-range diffusion, generally, the longer structure relaxation time t_α results in better glass forming ability, although the direct correlation between the dynamic heterogeneity and GFA is much complex. However, in the Cu-Zr-Ag system, the Ag addition does not result in longer t_α and, instead, a strong coupling between chemical and dynamic heterogeneities. Based on the microscopic dynamic theory, flow and structure changes in a supercooled liquid involve cooperative atomic motion.[26] A strong dynamic heterogeneity can induce divergence in the size of the cooperating regions. The coupling between chemical inhomogeneity and dynamic heterogeneity appears to promote the partitioning and fragmentation of dynamic processes, resulting in less cooperation between the slow-dynamics regions and the fast-dynamics regions. Since both slow- and fast-dynamics regions are much smaller than the critical size of crystallites, the spatial partitioning and dynamic isolation caused by the coupling may significantly retard the kinetics of crystallization of the supercooled liquid and leads to the improved GFA.

In summary, our molecular-dynamic simulation with EAM potentials reveals a strong coupling between chemical and dynamic heterogeneities in a multicomponent $Cu_{45}Zr_{45}Ag_{10}$ alloy, which appears to play a crucial role in the improved GFA by Ag addition. Because more or less chemical heterogeneity widely exists in multicomponent alloys, the dynamic coupling observed in this study may be a universal phenomenon in BMGs. This study may have an important implication in elucidating the dynamic origins of the BMG formation at a very low critical cooling rate.

This research was sponsored by Grants-in-Aid for scientific research from Kakenhi (Grant Nos. 20710080, 20226013), Global COE for Materials Research and Education, and the World Premier International Research Center Initiative program by MEXT, Japan. This research was also supported by the U.S. NSF under Grant No. DMR-0907325. We would like to thank the Center for Computational Materials Science, Institute for Materials Research, Tohoku University for providing us with the Hitachi SR11000 (model K2) supercomputing system.

*Corresponding author; mwchen@wpi-aimr.tohoku.ac.jp

[1] A. L. Greer, Science **267**, 1947 (1995).
[2] A. Inoue, Acta Mater. **48**, 279 (2000).
[3] D. B. Miracle, Nature Mater. **3**, 697 (2004).
[4] T. Egami, S. J. Poon, Z. Zhang, and V. Keppens, Phys. Rev. B **76**, 024203 (2007).
[5] H. W. Sheng, W. K. Luo, F. M. Alamgir, J. M. Bai, and E. Ma, Nature (London) **439**, 419 (2006).
[6] Y. Q. Cheng, E. Ma, and H. W. Sheng, Phys. Rev. Lett. **102**, 245501 (2009).
[7] A. R. Yavari, Nature (London) **439**, 405 (2006).
[8] X. K. Xi, L. L. Li, B. Zhang, W. H. Wang, and Y. Wu, Phys. Rev. Lett. **99**, 095501 (2007).
[9] T. Fujita, K. Konno, W. Zhang, V. Kumar, M. Matsuura, A. Inoue, T. Sakurai, and M. W. Chen, Phys. Rev. Lett. **103**, 075502 (2009).
[10] J. Kurchan, Nature (London) **433**, 222 (2005).
[11] P. G. Debenedetti and F. H. Stillinger, Nature (London) **410**, 259 (2001).
[12] H. Tanaka, J. Phys.: Condens. Matter **15**, L491 (2003).
[13] Y. Q. Cheng, E. Ma, and H. W. Sheng, Appl. Phys. Lett. **93**, 111913 (2008).
[14] S. M. Chathoth, B. Damaschke, M. M. Koza, and K. Samwer, Phys. Rev. Lett. **101**, 037801 (2008).
[15] Y. T. Shen, T. H. Kim, A. K. Gangopadhyay, and K. F. Kelton, Phys. Rev. Lett. **102**, 057801 (2009).
[16] S. J. Plimpton, J. Comput. Phys. **117**, 1 (1995).
[17] See supplementary material at http://link.aps.org/supplemental/10.1103/PhysRevB.81.140204 for additional information.
[18] J. L. Finney, Proc. R. Soc. London, Ser. A **319**, 479 (1970).
[19] W. Zhang and A. Inoue, J. Mater. Res. **21**, 234 (2006).
[20] C. Toninelli, M. Wyart, L. Berthier, G. Biroli, and J.-P. Bouchaud, Phys. Rev. E **71**, 041505 (2005).
[21] O. Dauchot, G. Marty, and G. Biroli, Phys. Rev. Lett. **95**, 265701 (2005).
[22] A. S. Keys, A. R. Abate, S. C. Glotzer, and D. J. Durian, Nat. Phys. **3**, 260 (2007).
[23] A. Widmer-Cooper, P. Harrowell, and H. Fynewever, Phys. Rev. Lett. **93**, 135701 (2004).
[24] A. Widmer-Cooper and P. Harrowell, Phys. Rev. Lett. **96**, 185701 (2006).
[25] G. A. Appignanesi, J. A. Rodriguez Fris, R. A. Montani, and W. Kob, Phys. Rev. Lett. **96**, 057801 (2006).
[26] G. Adam and J. H. Gibbs, J. Chem. Phys. **43**, 139 (1965).